ISSN 2179-3956

THE EFFECTS OF LUBRICATING OIL ADDITIVES ON THE ROLLING CONTACT FATIGUE STRENGTH OF A ROLLING BEARING FOR AN AUTOMATIC TRANSMISSION[1]

Toshihiko Ichihashi[2]
Hiroshi Fujita[2]
Susumu Matsumoto[3]

Abstract

The effects of lubricating oil additives on the pitting life of a radial needle bearing and a thrust needle bearing used for a transmission in passenger cars were investigated. Lubricating oil additives formed a tribofilm with tens of nanometers on the rolling surface of the needle bearing, and the difference in the pitting life of the radial needle bearing was about twice and that of the thrust needle bearing was about 30 times according to a lubricating oil additive. The pitting life was related to the hardness of the tribofilm; i.e., the pitting life grew longer as the tribofilm became softer.
Keywords: Lubricating oil; Bearing; Pitting; Tribofilm,

[1] *Technical contribution to the First International Brazilian Conference on Tribology – TriboBr-2010, November, 24th-26th, 2010, Rio de Janeiro, RJ, Brazil.*

[2] *Chief Researcher, Lubricants Research Laboratory Idemitsu Kosan Co.,Ltd., Chiba Japan.*

[3] *Professor of Waseda Univ. Graduate School of Information, Production and Systems, Fukuoka Japan.*

ISSN 2179-3956

1 INTRODUCTION

Recently, attempts to lower the viscosity of gear oils and automatic transmission fluids (ATFs) for passenger cars have been conducted in order to achieve better fuel economy. In general, when the viscosity of a lubricant is reduced, the pitting life of the gear and bearing tends to decrease. The decrease in the pitting life is prevented by optimizing additives mixed into lubricating oil and base oil.(1) However, from the viewpoint of saving resources, the miniaturization and longer lifetime of the transmission has been required, and further improvement of the pitting life has been expected.(2) In automatic transmissions, more than 20 bearings are used, and 80% of them are needle bearings. The needle bearings can be divided into a radial needle bearing and a thrust needle bearing according to the mechanism. The rolling surface of the radial needle bearing is thought to just roll. In the case of the thrust needle bearing, since motion slip is distributed in the direction of the needle axis, slippage must be considered in addition to rolling. Since the roll and slip characteristics of the radial needle bearing differ from those of the thrust needle bearing, differences in the effects of additives on the pitting life are thought to exist between the radial and thrust needle bearings.

Therefore, we investigated the effects of additives on the pitting life of a commercially available radial needle bearing, using some additives mixed with a mineral oil.(3) In the present study, we evaluated the effects of these additives on the pitting life of a thrust needle bearing. Moreover, we analyzed the chemical composition, thickness, and hardness of a tribofilm generated on the rolling surface, and the roughness of the counter surface in nanometer order. In this paper, we report the pitting lives of these two bearings, and discuss the relationship between these characteristics and the pitting life.

2 METHODS AND TEST OILS

2.1 Pitting Life Test

We manufactured radial and thrust needle bearing fatigue life testers for the pitting life test. Figure 1 show schematic diagrams of these testers and photographs of test bearings. In the radial needle bearing fatigue life tester (1), a radial needle bearing was installed on the drive shaft as the test bearing. The prescribed load was added on the jug that fixed the outer race of the bearing, and the bearing was rolled by the motor in the controlled-temperature oil bath. The pitting life of the test oil was determined by evaluating the pitting occurring on the bearing rolling surface.

In the thrust needle bearing fatigue life tester (2), a thrust needle bearing was

ISSN 2179-3956

installed on the drive shaft as the test bearing. The prescribed load was added on the jug that fixed the under race of the bearing, and the upper race was rolled by the motor in the controlled-temperature oil bath. The pitting life of the test oil was determined by evaluating the pitting occurring on the needle bearing rolling surface.

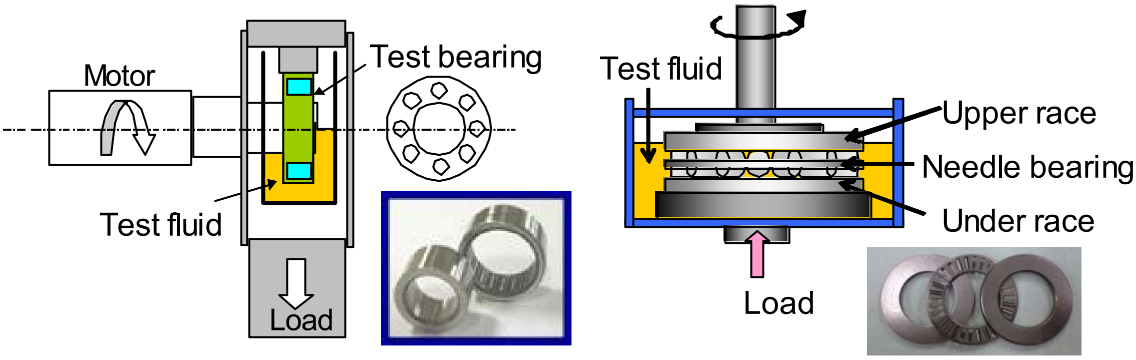

（1） Radial needle bearing (2) Thrust needle bearing

Figure 1. Main part of needle bearing fatigue life tester and test bearing

Table 1 shows the test conditions. The pitting life was determined to be between the initiation and the time when vibration suddenly increased. After the test was complete, the bearing was disassembled, and the pitting damage was confirmed to occur on the rolling surface. The load was raised from 0 to the prescribed load while the bearing was rolled, and the test load was kept until the damage occurred.

Table 1 Fatigue life test conditions

Tester	Radial needle bearing fatigue life tester		Thrust neeedle bearing fatigue life tester	
Bearing	Inner race	Drive:17mm dia., 10.2mm width	Upper race	Drive:39mm outer dia., 28 mm inner dia.
	Outer race	Driven:20mm dia., 10mm width	Under race	Driven:40mm ourterdia., 26.5mm inner dia.
	Needle	No. of needle 20	Needle	No. of needle 12
	Needle size	1.6mm dia.,6.8mm width	Needle size	2.0mm dia.,5.0mm width
	Material	Bearing steel (SUJ2)	Material	Bearing steel (SUJ2)
	Cage	Pressed steel	Cage	Pressed steel
	Radial clearance	0.02mm	Radial clearance	0.02mm
Lubrication	500ml	120 ℃	150ml	120 ℃
Test condition	Drive roller	2000rpm	Drive roller	1000rpm
Running in	0～4000N	60s	0～5880N	20s
Test	4000N		5880N	

2.2 Test Oils

Table 2 shows the chemical composition of test oils. Hydrocracked paraffinic mineral oil was used as the base oil, and seven compound oils were tested. These

ISSN 2179-3956

test oils were coded as test oils P, S, Ca, P+S, Ca+S, Ca+P, and Ca+P+S. P is tri-cresyle phosphate (TCP), S is dibenzyl disulfide (DBDS), and Ca is overbased calcium sulfonate (OBCS). When 0.3 mass% of TCP was mixed, the P content of the test oil became 0.025 mass%. When 0.2 mass% of DBDS was mixed, the S content of the test oil became 0.05 mass%. When 1.0 mass% of OBCS was mixed, the Ca content of the test oil became 0.15 mass%. These amounts of additives mixed with the base oil were determined by referring to the amounts of additives actually mixed with ATFs. Since the amount of additive added to the base oil was very small, the kinematic viscosities of the test oils used in this study were approximately the same.

Table 2 Chemical composition of test oils

mass%

Sample oil code	P	S	Ca	P+S	Ca+S	Ca+P	Ca+P+S
Mineral oil 150N	99.7	99.8	99.0	99.5	98.8	98.7	98.5
Tricresyl phosphate	0.3			0.3		0.3	0.3
Dibenzyl disulfide		0.2		0.2	0.2		0.2
Overbased calcium sulfonate			1.0		1.0	1.0	1.0

2.3 Analysis of the Rolling Surface

The rolling surface contact pressure was measured. Moreover, the state of the pitting was observed after the pitting life test was completed. The observation was performed using an optical microscope, scanning electron microscope (SEM), electron probe micro analyzer (EPMA), and X-ray photoelectron spectroscopy (XPS), and the state of the surface and near-surface was analyzed. In the case of using the thrust needle bearing, the test piece after the pitting test was investigated using a transmission electron microscope with focused ion beam (FIB-TEM). Namely, the test piece was cut in the depth direction using the ion beam, and the tribofilm generated on the cross section was directly observed using TEM. The hardness of the tribofilm was measured using a nano-indenter. The minute surface texture of the rolling surface after the pitting test was measured using an atomic force microscope (AFM).

3 RESULTS AND DISCUSSION

First, the results obtained by the pitting test using the radial needle bearing are described. And then, the results obtained by the pitting test using the thrust needle bearing are described, and the relationship between the tribofilm generated on the rolling surface and the fatigue life is examined.

ISSN 2179-3956

3.1 The Pitting Life and the Tribofilm of the Radial Needle Bearing

3.1.1 The pitting life of the radial needle bearing

Five tests were performed for each test oil, and the duration until pitting occurred was expressed in a Weibull distribution. Figure 2 shows the test results of test oils in pitting life at L_{50}, which is the cumulative damage at 50% on a Weibull plot.

The results obtained by using the radial needle bearing indicated that the pitting life decreased when the additives were mixed, compared with the base oil. The pitting life of test oil S was the shortest and decreased by approximately 60%, compared with the base oil. The pitting life of test oil P+S was the longest among all the test oils and almost equal to that of the base oil.

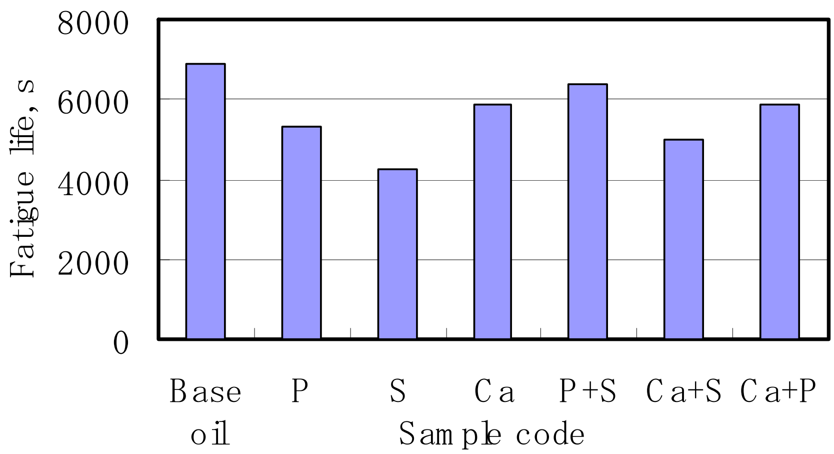

Figure 2. Results of pitting test with L_{50} Life.

3.1.2 Observation of the bearing rolling surface after the test

The bearing after the pitting life test was cut and its inside was observed. Since the section of the tester to be evaluated was of the cantilever type, exfoliation due to one-sided fatigue was observed on the outer race rolling surface. The exfoliation was located at the place, on which the maximum load was added during the test. Figure 3 shows the exfoliation state. When the load was actually added, the deflection was generated, and the edge release was generated. When the edge release was involved, the edge load at the edge was approximately 20% greater than that at the center of the roller. Actually, the pitting damage occurred at the place where the contact pressure was 3.6GPa which was reported with another paper.[3] Since the pitting life differed according to additive, the characteristics of the tribofilm were considered to affect the pitting life.

ISSN 2179-3956

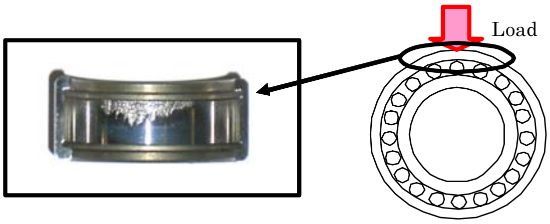

Figure 3. Optical photographs on outer race tested with oil P.

3.1.3 Analysis of the Tribofilm

The test was stopped at 2000 seconds after the initiation when no pitting occurred with any additive, and the outer race rolling surface of the bearing before the pitting occurrence was analyzed using XPS. The place for analysis was the upper edge of the outer race. Figure 4 shows the results of the measurement and analysis. The graphs in this figure show the changes in the ratio of the detected element against the depth from the surface. The chemical composition of the formed tribofilm was attributable to the additive in the test oil, and the compound was identified based on the binding energy of each element. It was confirmed that the film containing calcium oxide (CaO) was formed from test oil Ca, the film containing ferric phosphate ($Fe_3(PO_4)_2$) was formed from test oil P, the film containing ferrous sulfide (FeS) and ferrous sulfate ($FeSO_4$) was formed from test oil S, and the film containing $Fe_3(PO_4)_2$, FeS, and $FeSO_4$ was formed from test oil P+S.

Although the thicknesses of the films formed from test oils Ca and P were thicker than 100 nm, the thickness of the film formed from test oil S was as thin as 20 nm. Since the thickness of the film formed from test oil P+S was 50 nm, the thickness and chemical composition of the film formed from test oil P+S were in between those of test oils P and S. The difference in the film thickness did not directly relate to the duration of the pitting life. The duration of the pitting life was considered to relate to chemical characteristics or physical properties of the tribofilm.

Sample code		Ca	P	S	P+S
Depth profile	Before pitting 2000s	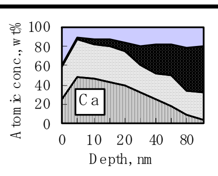	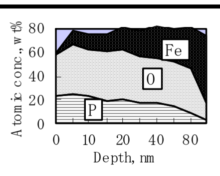	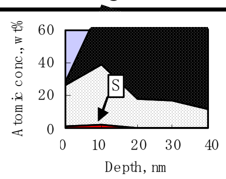	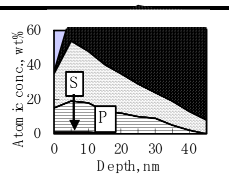
Composition		CaO	$Fe_3(PO_4)_2$	FeS,$FeSO_4$	$Fe_3(PO_4)_2$,FeS,$FeSO_4$
Film thick ,nm	Before	120	110	20	P:50, S:15
	After	125	140	50	P:120, S:30
Fatigue life, s		5886	5304	4260	6381

Figure 4. Structure of tribofilm on outer race.

ISSN 2179-3956

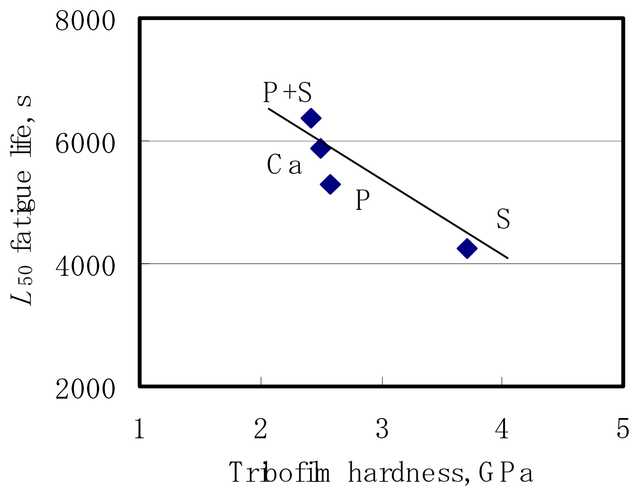

Figure 5. Relation between fatigue life and hardness of tribofilm

Therefore, the hardness of four tribofilms shown in Figure 4 was measured using a nano-indenter. The measurement conditions included the indentation load of 100 Nm and the indentation depth of 20 nm. Six points were measured on the bearing outer race before the occurrence of pitting (2000 s), and the average of the obtained values was calculated. Figure 5 shows the relationship between the obtained hardness of the tribofilm and the pitting life. As shown in this figure, the relationship between them was confirmed to exist, and the softer film tended to extend the pitting life.

3.2 The Pitting Life and the Tribofilm of the Thrust Needle Bearing

3.2.1 The pitting life of the thrust needle bearing

Figure 6 shows the pitting test results of test oils obtained by using the thrust needle bearing fatigue life tester. The pitting life was expressed as the cumulative cycle of drive shaft until pitting occurred in Weibull distribution. Figure 7 shows the test results of test oils in pitting life at L_{50}. As shown in Figure 7, the cumulative cycle of test oil P was 12.3 × 10^6, and extremely larger than that of the base oil. The cumulative cycle of test oil Ca was 5.6 × 10^6, and similar to that of the base oil. The cumulative cycle of test oil S was 0.45 × 10^6, extremely smaller than that of the base oil. It was revealed that the effects of additives on the fatigue life were greater in the thrust needle bearing than in the radial needle bearing.

ISSN 2179-3956

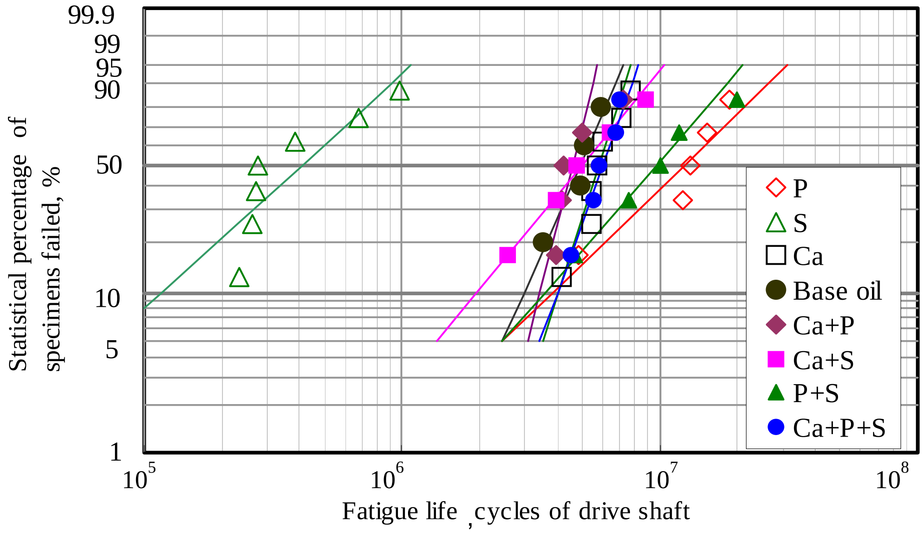

Figure 6. Pitting test results of additive oil.

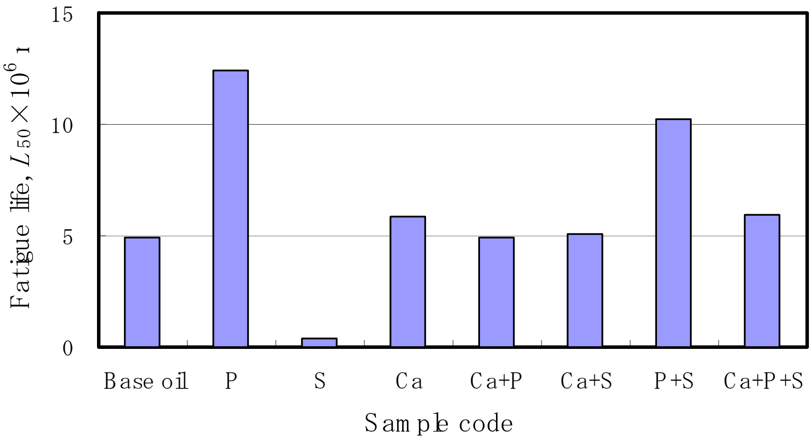

Figure 7. Results of pitting test with L_{50} Life.

3.2.2 Observation of the bearing rolling surface and the friction conditions

Figure 8 shows optical photographs of needles after the test. The upper photographs show the overall appearance and the lower photographs show the magnified pitting damage. The place on which pitting occurred tended to differ according to test oil. When the base oil, test oil P, and Ca were used, pitting occurred at the outer part of the needle bearing. Pitting occurred at the inner part only when test oil S was used.

Since the one tip of the pitting damage was sharply exfoliated and the other tip was deformed, the characteristics of surface origin pitting remarkably appeared. Almost all of the pitting was considered to be of surface origin. The contact pressure was calculated, and the maximum Hertz contact pressure was 1.79 GPa.

ISSN 2179-3956

In the case of the thrust needle bearing, since the needle rotates and revolves around the central axis of the bearing, a spin motion is generated on the orbital planes of the upper and under races.(4) Pitting is considered to occur at the outside from the center where the sliding distance becomes longer under the same friction conditions. Actually, pitting occurred at the outside from the center of the needle for all the test oils except test oil S. When test oil S was used, pitting occurred at the inside from the center of the needle.

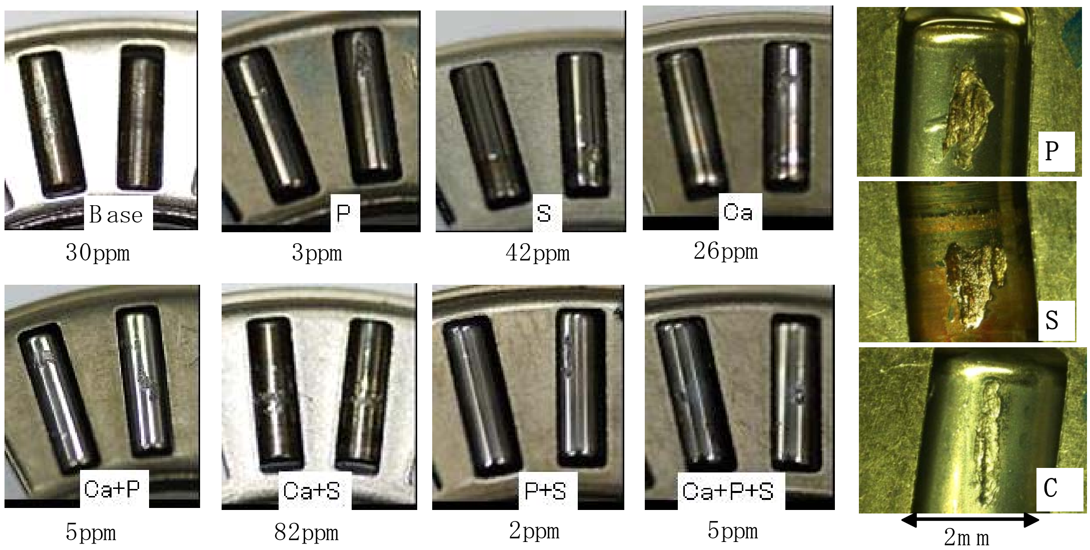

Figure 8. Optical photographs of needles and iron ion concentration of the oils after test.

3.2.3 The relationship between the tribofilm and the pitting life

Table 3 shows the results obtained by XPS. Since the tribofilm thicknesses of test oils S, P, and P+S were 40–50 nm, Ca+P and Ca+P+S exceeded 130 nm. Since the tribofilm thicknesses of test oils Ca and Ca+S were 80–130 nm, relatively thick tribofilms were formed.

Table 3. Properties of tribofilm by XPS.

Sample oil code	P	S	Ca	P+S	Ca+S	Ca+P	Ca+P+S
Chemical species	$FePO_4$ $Fe_3(PO_4)_2$	FeS	CaO	$FePO_4$ $Fe_3(PO_4)_2$	CaO	CaO $FePO_4$	CaO $FePO_4$
nm	40	40	80	50	130	Over130	Over130

The chemical compositions of tribofilms formed when the compound oils with a single additive were used were similar to those identified in the radial needle bearing pitting test, thus generating calcium oxide, ferric phosphate, and ferrous sulfide. Test oil Ca+S generated calcium oxide. Test oil P+S generated ferric phosphate. The reason why ferrous sulfide was not detected is considered to be that since the reactivity of the sulfur-based additive was lower than that of the calcium- or

ISSN 2179-3956

phosphorus-based additive, the sulfur-based additive scarcely reacted under these test conditions.(5) To supplement the results of XPS measurements, the tribofilm was directly observed using FIB-TEM when test oil P, S, or Ca was used. Figure 9 shows the cross-sectional FIB-TEM micrographs of the tribofilms.

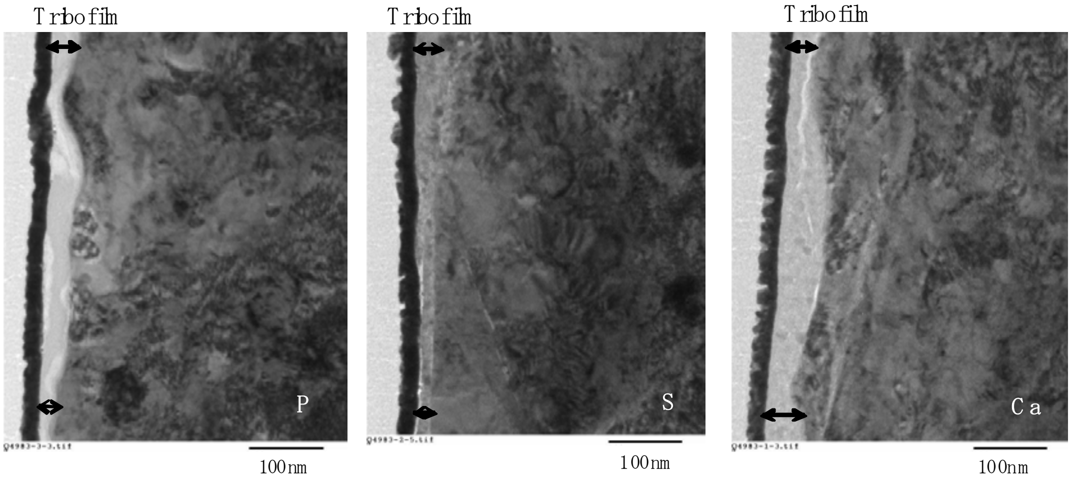

Figure 9. Cross-sectional FIB-TEM micrographs of the tribofilms.

The dark part with approximately 10 nm width at the left side of each photograph is a gold evaporated film to protect the surface when cutting. The white part at the right side of the gold evaporated film is the tribofilm. The base material is seen at the right part of each photograph. The elements composing each part were confirmed by an elementary analysis using an energy dispersive X-ray spectroscopy (EDS). The components of each additive were detected from the tribofilm.

The tribofilm thickness measured using TEM was 20−50 nm when test oil P or S was used and 20−80 nm when test oil Ca. The results obtained using TEM were similar to those obtained using XPS. During the pitting test, the tribofilms with the thicknesses between a few nm and exceeding 100 nm were confirmed to be formed by each additive. A special correlation between the pitting life and the tribofilm thickness could not be found.

3.2.4 The Hardness of the tribofilm

The tribofilm was considered to affect the duration of the pitting life, and it was measured using a nano-indenter. Figure 10 shows the relationship between the obtained tribofilm hardness and the pitting life. As shown in this figure, the tribofilm tended to be softer with longer pitting life. This tendency was similar to that of the radial needle bearing.

ISSN 2179-3956

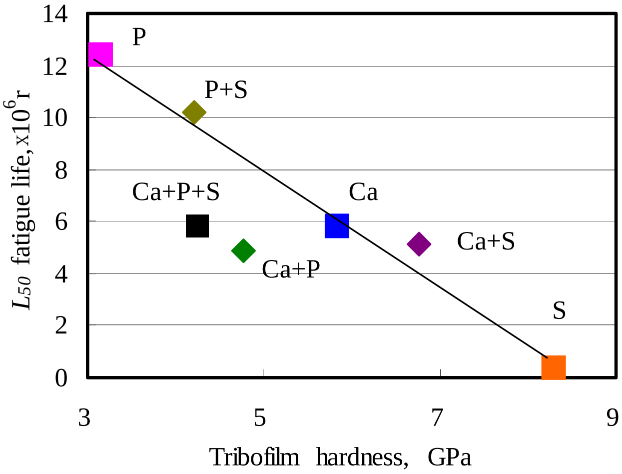

Figure 10. Relationship between the fatigue life and the hardness of tribofilm.

3.2.5 Factors of the tribofilm that affect the fatigue life

Although the tribofilm tended to be softer with longer pitting life, two points of test oils Ca+P and Ca+P+S were below the approximation line. The reason for this was considered to be that some characteristics affected this tendency. Then, the surface shape of the tribofilm of the under race, which contacted with the needle bearing, was measured using AFM. Figure 11 shows the arithmetic mean roughness (Ra) of each surface in nanometer order. The Ra value was obtained by averaging the measurements of five surfaces, on which no large wear trace was observed. As shown in Figure 11, the Ra value of the tribofilm, which contained the Ca-based additive, tended to be large, and the surfaces of tribofilms formed with test oils Ca+P+S and Ca+P were particularly rough. Since wear of the rolling surface was considered to affect the duration of the pitting life, the iron ion concentration in the test oil after the pitting life test was showed in Figure 8. The detected iron ion concentration was divided by the test duration of each test oils to compare the iron ion concentration per unit time. Consequently, it was revealed that wear was 5−500 times larger when test oil S was used than when the other test oils were used.

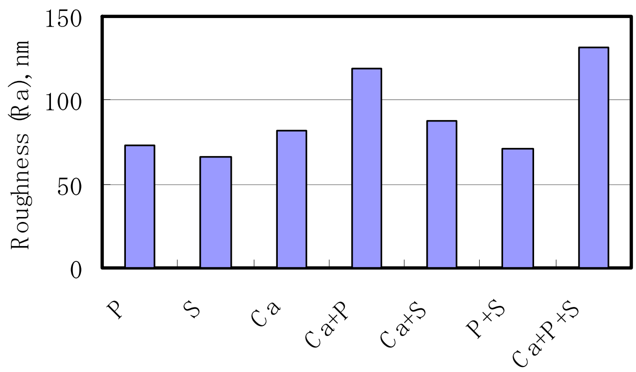

Figure 11. Roughness of tribofilm by AFM.

ISSN 2179-3956

Then, the relationship between the pitting life and the tribofilm performance, in which wear characteristics were added to the hardness of the tribofilm and its surface ruggedness, was examined. Figure 12 shows the result of the examination. As shown in this figure, [the tribofilm hardness × the surface roughness (*Ra*) × $(\text{wear})^{1/3}$] could be used as the index for the pitting life L_{50}. Since the 1/3 power of wear was considered as the length of wear, the tribofilm in nanometer order was more fragile and a crack, which would become the origin of pitting, more easily occurred as the tribofilm was harder and the surface was rougher. Moreover, when wear was large, the stable tribofilm was not formed. Therefore, the relaxation effect of stress due to the tribofilm was insufficiently displayed, and pitting occurred in an early stage. Unlike the radial needle bearing, the effect of motion slip in addition to that of rolling friction must be taken into consideration for the thrust needle bearing. Moreover, roughness and wear of the counter surface, which remarkably affects the lubricated state of motion slip, must be added to the index of the pitting life.

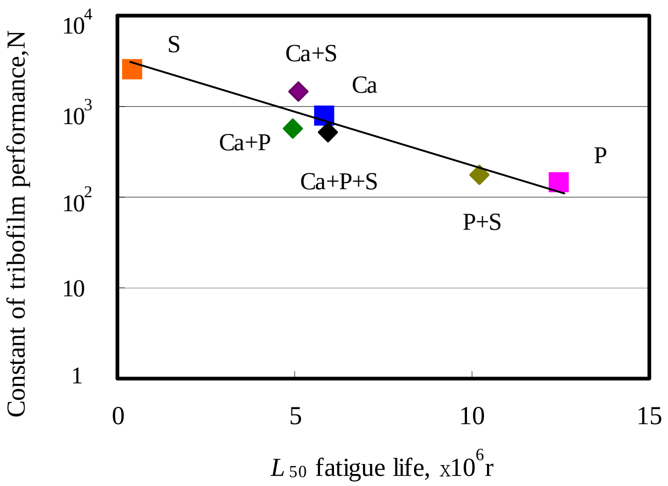

Figure 12. Relation between fatigue life and tribofilm performance.

4 CONCLUSION

The difference in the pitting life according to additive was confirmed by the pitting life test using radial and thrust needle bearings, and the relationship between the pitting life and the tribofilm was examined as follows:

(1) Phosphorus-, sulfur-, and calcium-based additives formed tribofilms with 20−150 nm thickness on the rolling surface of the needle bearing. The characteristics of the formed tribofilm affected the duration of the pitting life. The pitting life (operating time) differed approximately 2 and 30 times according to additive in radial and thrust needle bearings, respectively.

(2) An additive with a longer pitting life was formed softer tribofilm on both radial and thrust needle bearings except base oil which does not produce tribofilm. The pitting

ISSN 2179-3956

life was the longest when a phosphorus-based additive was combined with a sulfur-based additive.

(3) Since the slip ratio of the rolling surface was larger in the thrust needle bearing than in the radial needle bearing, surface factors which are easily affected by sliding friction must be taken into consideration. As an evaluation factor, [the tribofilm hardness × the surface roughness (*Ra*) × $(\text{wear})^{1/3}$] was extracted. When this value was smaller, the pitting life was longer.

(4) To improve the rolling contact fatigue strength, lubricating oil, in which a phosphorus-based additive was combined with a sulfur-based additive, was effective. A soft and smooth tribofilm with low wear was also effective.

REFERENCES

1 I. Kurihara and O. Kurosawa: Design and Performance of Low-Viscosity ATF, SAE Tech Pap. SAE-2007-01-3974 (2007).

2 H. Fujita, Y. Takakura and T. Ikeda: Study of Low Viscosity ATF with Extending Gear Fatigue Life, SAE Tech Pap. SAE-2007-01-1976 (2007).

3 T. Ichihashi, M. Yokomizo and S. Matsumoto: Investigation of Fatigue Life of Lubricating Oil Additives Using Radial Needle Bearing Test, Proceedings of MPT2009-Sendai, JSME International Conference on Motion and Power Transmissions May-13-15, (2009), 519−523.

4 J. Brandlein, L. Hasbargen, P. Eschmann and K. Weigand: Die walzlagerpraxis, Vereinigte Fachverlage GmbH, Mainz, p. 95, (1995).

5 H. P. Nixon: Effects of Extreme Pressure Additives in Lubricants on Bearing Fatigue Life, Iron and Steel Engineer, pp. 21−26, December (1998).